Available online at www.sciencedirect.com

ScienceDirect

Mendeleev Commun., 2022, **32**, 576–578

Mendeleev Communications

Synthesis, structure and catalytic properties of Pd^{II}-based bimetallic complexes with ferrocenecarboxylic acid

Anna S. Popova,[a,b] Nadezhda K. Ogarkova,[a] Sergey S. Shapovalov,[b] Ivan V. Skabitsky,[b] Ekaterina K. Kultyshkina,[a] Ilya A.Yakushev*[b] and Michael N. Vargaftik[b]

[a] *Peoples Friendship University of Russia (RUDN University), 117198 Moscow, Russian Federation*
[b] *N. S. Kurnakov Institute of General and Inorganic Chemistry, Russian Academy of Sciences, 119991 Moscow, Russian Federation. E-mail: ilya.yakushev@igic.ras.ru*

DOI: 10.1016/j.mencom.2022.09.002

Novel highly soluble palladium-based complexes with ferrocenecarboxylic acid of general formula $[Pd(lut)_2(FcCOO)_2]$ (lut is 2,6- or 3,4-lutidines) were synthesized and structurally characterized by single-crystal X-ray diffraction. The catalytic oxidation of 1,2-diphenylacetylene with these complexes gave dibenzo[*a*,*e*]pentalene derivative along with other products.

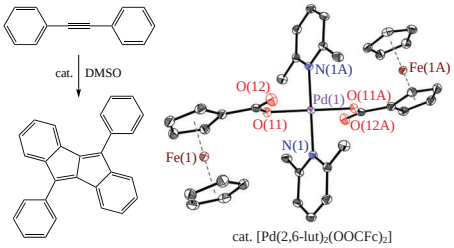

Keywords: palladium complexes, ferrocenecarboxylic acid, ligand exchange, XRD analysis, homogeneous catalysis, diphenylacetylene, dibenzo[*a*,*e*]pentalene.

Heterometallic compounds are known to be widely used as homogeneous catalysts for hydrogenation and isomerization of unsaturated hydrocarbons,[1–3] oxidation of alcohols,[4] as well as precursors of metal-oxide materials[5] and supported catalytic systems for selective hydrogenation[6] and oxygen reduction.[7] Moreover, palladium complexes are employed in hydroboration and hydroformylation of styrene,[8] polymerization of norbornene derivatives[9] and diazoacetates.[10] The inclusion of organometallic carboxylic acids, *e.g.* cymantrenecarboxylic,[11] or, in particular ferrocenecarboxylic acids, into the composition of compounds is an affordable way to obtain precursors of catalytically active heterometallic materials and nanoparticles.[12] Carboxylate complexes are best suited for these purposes because they do not contain strongly coordinated and hard-to-remove ligands based on sulfur, phosphorus, *etc*.

Previously, the possibility of synthesizing palladium(II) complexes $[Pd(Py)_2(FcCOO)_2]$ and $[Pd(Phen)(FcCOO)_2]$ from palladium(II) acetate $[Pd_3(OAc)_6]$, which can potentially be used to obtain bimetallic nanosized phases, was shown.[13] However, the previously obtained compounds possessed very low solubility in most applicable solvents, and their use in homogeneous catalysis is unpromising. Therefore, in this work, we propose a two-stage synthesis (Scheme 1) of soluble bimetallic palladium complexes $[Pd(lut)_2(FcCOO)_2]$ (lut is 2,6- or 3,4-lutidine).

The reaction of palladium acetate with lutidines (stage i) under mild conditions[14] results in mononuclear *trans*-complexes

$$[Pd_3(OAc)_6] + 6\,lut \xrightarrow{i} 3[Pd(lut)_2(OAc)_2]$$
1, **2**

$$[Pd(lut)_2(OAc)_2] + 2\,FcCOOH \xrightarrow{ii} [Pd(lut)_2(FcCOO)_2] + 2\,AcOH$$
3, **4**

1, **3** lut = 2,6-lutidine
2, **4** lut = 3,4-lutidine

Scheme 1 *Reagents and conditions*: i, PhH, room temperature, slow evaporation; ii, CH_2Cl_2, MeOH (for **3**), room temperature.

$[Pd(lut)_2(OAc)_2]$ **1**, **2** structurally similar to other palladium complexes with aromatic monodentate N-donors.[15] Thereafter acetate anions can be easily replaced by ferrocenecarboxylate anions (stage ii) to afford crystalline products **3**, **4** (see Scheme 1). Remarkably, in contrast to analogous compounds with pyridine ligands,[13] the resulting complexes **3**, **4** do not contain any solvate molecules in their crystal structure according to XRD studies. Heteroanionic structures, products of partial substitution of acetate anions, are not formed as well. X-ray diffraction study† showed that complexes **1**–**4** (Figures S1, S2 of Online Supplementary Materials and Figures 1, 2) have usual square-planar Pd^{II} moiety as a core unit, surrounded by two

† *Crystal data for* **1**. $C_{18}H_{24}N_2O_4Pd$, M = 438.79, triclinic, a = 8.367(2), b = 8.394(3) and c = 8.473(3) Å, α = 89.949(8)°, β = 61.222(7)°, γ = 63.451(7)°, V = 448.8(2) Å^3, space group $P\bar{1}$, Z = 1, d_{calc} = 1.623 g cm^{-3}, $F(000)$ = 224, $\mu(MoK_\alpha)$ = 1.059, yellow prism with dimensions *ca.* 0.33 × 0.25 × 0.18. Total of 6813 reflections (2752 unique, R_{int} = 0.017) were measured using ω- and φ-scan modes at 100 K. The final residuals were: R_1 = 0.0156 for 2744 reflection with $I > 2\sigma(I)$ and wR_2 = 0.0415 for all data and 118 parameters. GoF = 1.136.

Crystal data for **2**. $C_{18}H_{24}N_2O_4Pd$, M = 438.79, triclinic, a = 7.2081(2), b = 7.6808(2) and c = 9.2124(3) Å, α = 75.916(1)°, β = 67.741(1)°, γ = 85.735(1)°, V = 457.75(2) Å^3, space group $P\bar{1}$, Z = 1, d_{calc} = 1.592 g cm^{-3}, $F(000)$ = 224, $\mu(MoK_\alpha)$ = 1.038, yellow prism with dimensions *ca.* 0.21 × 0.15 × 0.10. Total of 7762 reflections (2816 unique, R_{int} = 0.0204) were measured using ω- and φ-scan modes at 100 K. The final residuals were: R_1 = 0.0172 for 2802 reflection with $I > 2\sigma(I)$ and wR_2 = 0.0424 for all data and 118 parameters. GoF = 1.110.

Crystal data for **3**. $C_{36}H_{36}Fe_2N_2O_4Pd$, M = 778.77, monoclinic, a = 9.8707(2), b = 11.0262(2) and c = 14.3690(4) Å, β = 100.8298(11)°, V = 1536.02(6) Å, space group $P2_1/n$, Z = 2, d_{calc} = 1.684 g cm^{-3}, $F(000)$ = 792, $\mu(MoK_\alpha)$ = 1.555, yellow prism with dimensions *ca.* 0.24 × 0.23 × 0.05. Total of 25123 reflections (4733 unique, R_{int} = 0.0286) were measured using ω- and φ-scan modes at 100 K. The final residuals were: R_1 = 0.0257 for 4362 reflections with $I > 2\sigma(I)$ and wR_2 = 0.0686 for all data and 207 parameters. GoF = 1.078.

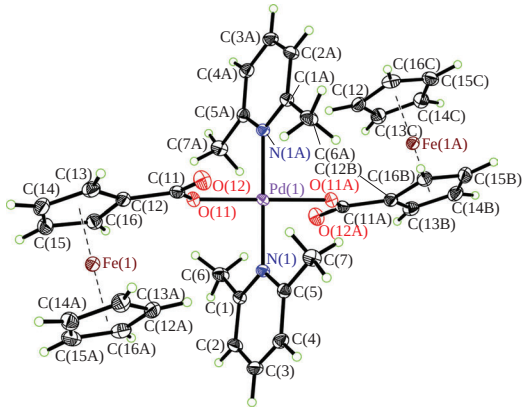

Figure 1 Molecular structure of complex $[Pd(2,6\text{-lut})_2(FcCOO)_2]$ **3**. Thermal ellipsoids are drawn at 50% probability level. Main geometrical parameters: Pd(1)–O(11) 2.0091(12) Å, Pd(1)–N(1) 2.0398(14) Å; $O(11)^{\#1}$–Pd(1)–O(11) 180.0°, $O(11)^{\#1}$–Pd(1)–N(1) 91.68(5)°, O(11)–Pd(1)–N(1) 88.32(5)°, $O(11)^{\#1}$–Pd(1)–$N(1)^{\#1}$ 88.32(5)°, O(11)–Pd(1)–$N(1)^{\#1}$ 91.68(5)°, N(1)–Pd(1)–$N(1)^{\#1}$ 180.0°. Symmetry transformations used to generate equivalent atoms:$^{\#1}$ $-x+1, -y+1, -z+1$.

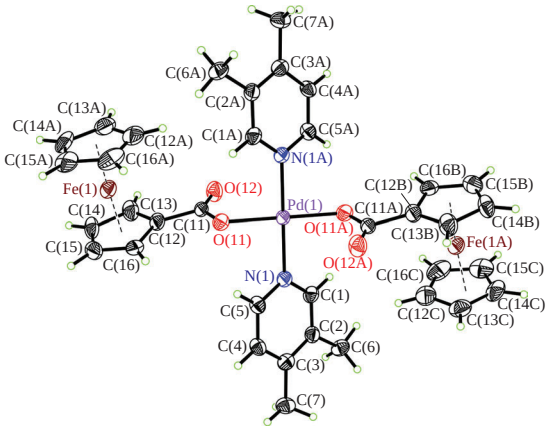

Figure 2 Molecular structure of complex $[Pd(3,4\text{-lut})_2(FcCOO)_2]$ **4**. Thermal ellipsoids are drawn at 50% probability level. Main geometrical parameters: Pd(1)–O(11) 2.016(5) Å, Pd(1)–N(1) 2.025(5) Å; $O(11)^{\#1}$–Pd(1)-O(11) 180.0°, $O(11)^{\#1}$–Pd(1)–N(1) 91.9(2)°, O(11)–Pd(1)–N(1) 88.1(2)°, $O(11)^{\#1}$–Pd(1)–$N(1)^{\#1}$ 88.1(2)°, O(11)–Pd(1)–$N(1)^{\#1}$ 91.9(2)°, N(1)–Pd(1)–$N(1)^{\#1}$ 180.0°. Symmetry transformations used to generate equivalent atoms:$^{\#1}$ $-x+2, -y+1, -z+1$.

oxygen and two nitrogen atoms in *trans*-positions each [Pd(1)–O(11) and Pd(1)–N(1) distances are 2.0090(12)–2.0247(10) and 2.0233(10)–2.0482(11) Å, respectively]. The central palladium atom in crystals **1**–**4** occupies the inversion centre of the unit cells, hence there is no deviation of Pd atoms from the O(11)–O(11A)–N(1)–N(1A) mean plane. It should be noted that other types of secondary interatomic intramolecular interaction involving the Pd atom, due to relatively long Pd(1) to carbonyl oxygen atom O(12) distance in both bimetallics **3** and **4** are unlikely to be strong in the solid phase [Pd(1)–O(12) is 3.0521(14) and 3.036(5) Å for **3** and **4**, respectively]. However, these distances are less than the sum of the Van der Waals radii of palladium and oxygen.[15] Despite of the presence of relatively bulky ferrocenyl fragments in the structures, in general, the palladium core environment corresponds to the molecular geometry characteristic of typical palladium carboxylate complexes.[16,17]

Complexes **1**–**4** were tested as catalytically active species in the model oxidation of 1,2-diphenylacetylene into benzil (1,2-diphenylethane-1,2-dione) **5** or 2,3-diphenyl-1-indenone **6** (Scheme 2). Surprisingly, these heteronuclear complexes have demonstrated the highest selectivity in one more reaction, namely, oxidation of the substrate *via* C–H activation route to afford 5,10-diphenyldibenzo[*a*,*e*]pentalene **7** (for its X-ray structure,† see Figure 3). Hydrocarbon **7** is known for its electrical properties and applications in organic thin-film

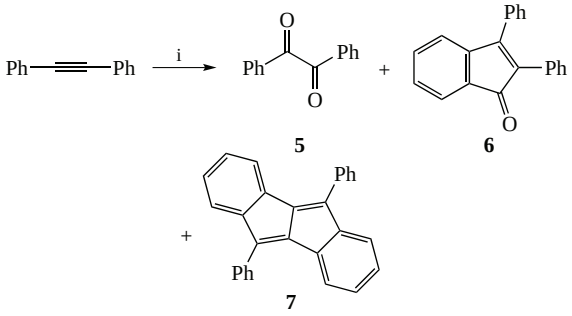

Scheme 2 *Reagents and conditions*: i, [Pd] catalyst, DMSO, 95 °C, 66–162 h.

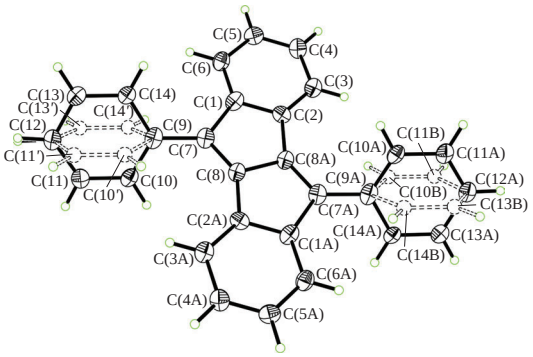

Figure 3 Molecular structure of 5,10-diphenyldibenzo[*a*,*e*]pentalene **7**. Thermal ellipsoids are drawn at 40% probability level.

Crystal data for **4**. $C_{36}H_{36}Fe_2N_2O_4Pd$, $M = 778.77$, triclinic, $a = 5.9190(17)$, $b = 8.7586(11)$ and $c = 15.725(5)$ Å, $\alpha = 105.717(3)°$, $\beta = 94.526(15)°$, $\gamma = 97.137(7)°$, $V = 773.2(3)$ Å^3, space group $P\bar{1}$, $Z = 1$, $d_{calc} = 1.672$ g cm^{-3}, $F(000) = 396$, μ(synchrotron radiation) = 1.743, yellow nugget with dimensions *ca*. $0.06 \times 0.04 \times 0.02$. Total of 11606 reflections (2959 unique, $R_{int} = 0.1010$) were measured using φ-scan mode at 100 K. The final residuals were: $R_1 = 0.0563$ for 2051 reflections with $I > 2\sigma(I)$ and $wR_2 = 0.1527$ for all data and 207 parameters. GoF = 1.018.

Crystal data for **7**. $C_{28}H_{18}$, $M = 354.42$, monoclinic, $a = 23.126(5)$, $b = 4.8853(9)$ and $c = 18.788(4)$ Å, $\beta = 122.597(7)°$, $V = 1788.3(7)$ Å^3, space group $C2/c$, $Z = 4$, $d_{calc} = 1.316$ g cm^{-3}, $F(000) = 744$, $\mu(MoK_\alpha) = 0.075$, red plate with dimensions *ca*. $0.08 \times 0.04 \times 0.02$. Total of 4925 reflections (1567 unique, $R_{int} = 0.1149$) were measured using ω- and φ-scan modes at 150 K. The final residuals were: $R_1 = 0.0698$ for 669 reflections with $I > 2\sigma(I)$ and $wR_2 = 0.1685$ for all data and 164 parameters. GoF = 0.930.

For crystals **1**–**3** and **7**, the reflections were collected on a Bruker D8 Venture diffractometer (graphite monochromatized MoK_α radiation, $\lambda = 0.71073$ Å). For crystal **4**, the reflections were collected using Rayonix SX165 CCD one-circle diffractometer at the 'Belok' beamline[18] of the National Research Center 'Kurchatov Institute' (Moscow, Russian Federation, synchrotron focusing-mirror monochromatized radiation, $\lambda = 0.74500$ Å). The reflection intensity was corrected for absorption using SADABS[19] and XDS software[20] (for **4** only). The structures were solved by direct methods[21] and refined by full-matrix least-squares technique[22] on F^2 with anisotropic displacement parameters for non-hydrogen atoms. The hydrogen atoms were placed in calculated positions and refined using a riding model with fixed isotropic displacement parameters [$U_{iso}(H) = 1.5\,U_{eq}(C)$ for methyl groups and $U_{iso}(H) = 1.2\,U_{eq}(C)$ for all other H-atoms]. All calculations were carried out using the SHELXTL[19] program and Olex2 X-ray data visualization program package[23]. For details, see Online Supplementary Materials, Table S1.

CCDC 2158137–2158141 contain the supplementary crystallographic data for this paper. These data can be obtained free of charge from The Cambridge Crystallographic Data Centre *via* http://www.ccdc.cam.ac.uk.

Table 1 Catalytic activity of palladium complexes in the transformation of 1,2-diphenylacetylene into compounds **5**–**7**.

Catalyst	*t*/h	Substrate conversion (%)	Products		
			5	**6**	**7**
$[Pd(2,6\text{-lut})_2(OAc)_2]$ **1**	66	75	+	+	+
$[Pd(3,4\text{-lut})_2(OAc)_2]$ **2**	162	64	+	+	+
$[Pd(Py)_2(FcCOO)_2]$	insoluble	0	0	0	0
$[Pd(Py)_2(OAc)_2]$	135	75	+	+	+
$[Pd(2,6\text{-lut})_2(FcCOO)_2]$ **3**	159	42	<1%	<1%	+
$[Pd(3,4\text{-lut})_2(FcCOO)_2]$ **4**	159	40	<1%	<1%	+

transistors.[24] Typically, synthesis of such compounds is carried out *via* the lithium-mediated reductive cyclization of *o*,*o*′-bis(arylcarbonyl)diphenylacetylenes,[25] reductive annulation of 1-phenyl-2-isopropylsilylacetylene[26] as well as C–H activation of diphenylacetylene.[27] In the last case, *o*-chloranil was used as an oxidizing agent and $PdCl_2$–AgOTf mixed salt system served as the catalyst.

In our investigation, two mixed-metal complexes **3** and **4** revealed unexpected selectivity toward 5,10-diphenyldibenzo[*a*,*e*]pentalene **7** while monometallic compounds showed only higher activity and conversion rate in the reaction discussed (see Scheme 2). However, in all cases mixtures of all three products **5**–**7** were formed (Table 1). The mechanism of formation of product **7** is probably similar to the mechanism proposed for a similar reaction in the presence of $PdCl_2$/AgOTf/*o*-chloroanil.[27] C–H palladation of phenyl ring *ortho*-directed by coordination to acetylene is followed by triple bond insertion of the second diphenylacetylene molecule into the Pd–C bond. Subsequently, intramolecular triple bond insertion and the second o*rtho* C–H palladation occur followed by reductive elimination of product **7** from Pd complex. The oxidation of the palladium complex, which completes the catalytic cycle, is possibly promoted by air oxygen. Thus, the formation of pentalene is favored in the presence of ferrocenyl carboxylate, probably due to its stronger basicity facilitating the C–H activation steps.

This study was supported by the Russian Science Foundation (grant no. 18-73-10206-P). The research was performed using the equipment of the JRC PMR IGIC RAS.

Online Supplementary Materials

Supplementary data associated with this article can be found in the online version at doi: 10.1016/j.mencom.2022.09.002.

References

1 I. P. Stolarov, I. A. Yakushev, A. V. Churakov, N. V. Cherkashina, N. S. Smirnova, E. V. Khramov, Y. V. Zubavichus, V. N. Khrustalev, A. A. Markov, A. P. Klyagina, A. B. Kornev, V. M. Martynenko, A. E. Gekhman, M. N. Vargaftik and I. I. Moiseev, *Inorg. Chem.*, 2018, **57**, 11482.
2 P. Buchwalter, J. Rosé and P. Braunstein, *Chem. Rev*., 2015, **115**, 28.
3 P. V. Markov, G. O. Bragina, A. V. Rassolov, I. S. Mashkovsky, G. N. Baeva, O. P. Tkachenko, I. A. Yakushev, M. N. Vargaftik and A. Yu. Stakheev, *Mendeleev Commun.*, 2016, **26**, 494.
4 (*a*) J. L. Kuiper and P. A. Shapley, *J. Organomet. Chem.*, 2007, **692**, 1653; (*b*) O. A. Nikonova, M. Capron, G. Fang, J. Faye, A.-S. Mamede, L. Jalowiecki-Duhamel, F. Dumeignil and G. A. Seisenbaeva, *J. Catal*., 2011, **279**, 310.
5 N. Yu. Kozitsyna, S. E. Nefedov, I. A. Yakushev, Z. V. Dobrokhotova, M. N. Vargaftik and I. I. Moiseev, *Mendeleev Commun.*, 2007, **17**, 261.
6 (*a*) N. S. Smirnova, E. V. Khramov, I. P. Stolarov, I. A. Yakushev, G. N. Baeva, G. O. Bragina, E. V. Belova, A. V. Ishchenko, A. S. Popova, Y. V. Zubavichus, M. N. Vargaftik and A. Yu. Stakheev, *Intermetallics*, 2021, **132**, 107160; (*b*) A. Yu. Stakheev, N. S. Smirnova, D. S. Krivoruchenko, G. N. Baeva, I. S. Mashkovsky, I. A. Yakushev and M. N. Vargaftik, *Mendeleev Commun.*, 2017, **27**, 515.
7 V. A. Grinberg, N. A. Mayorova, A. A. Pasynsky, A. A. Shiryaev, V. V. Vysotskii, I. P. Stolarov, I. A. Yakushev, N. V. Cherkashina, M. N. Vargaftik, Y. V. Zubavichus and A. L. Trigub, *Electrochim. Acta*, 2019, **299**, 886.
8 I. P. Beletskaya, C. Nájera and M. Yus, *Russ. Chem. Rev.*, 2020, **89**, 250.
9 G. O. Karpov and M. V. Bermeshev, *Dokl. Chem.*, 2020, **495**, 195 (*Dokl. Ross. Akad. Nauk, Ser. A*, 2020, **495**, 21).
10 I. V. Nazarov, E. V. Bermesheva, K. V. Potapov, Z. B. Khesina, M. M. Il'in, E. K. Melnikova and M. V. Bermeshev, *Mendeleev Commun.*, 2021, **31**, 690.
11 S. S. Shapovalov and I. V. Skabitsky, *Russ. J. Coord. Chem.*, 2021, **47**, 330 (*Koord. Khim.*, 2021, **47**, 288).
12 S. Tanaka and K. Mashima, *Inorg. Chem.*, 2011, **50**, 11384.
13 I. A. Yakushev, M. A. Dyuzheva, I. A. Stebletsova, A. B. Kornev, N. V. Cherkashina and M. N. Vargaftik, *Russ. J. Coord. Chem.*, 2022, **48**, 153 (*Koord. Khim.*, 2022, **48**, 157).
14 T. A. Stephenson, S. M. Morehouse, A. R. Powell, J. P. Heffer and G. Wilkinson, *J. Chem. Soc.*, 1965, 3632.
15 S. Alvarez, *Dalton Trans.*, 2013, **42**, 8617.
16 S. B. Halligudi, K. N. Bhatt, N. H. Khan, R. I. Kurashy and K. Venkatsubramanian, *Polyhedron*, 1996, **15**, 2093.
17 A. Shibatani, Y. Kataoka and Y. Ura, *Asian J. Org. Chem.*, 2021, **10**, 3285.
18 R. D. Svetogorov, P. V. Dorovatovskii and V. A. Lazarenko, *Cryst. Res. Technol*., 2020, **55**, 1900184.
19 *APEX3, SAINT and SADABS*, Bruker AXS, Madison, WI, 2016.
20 W. Kabsch, *Acta Crystallogr.*, 2010, **D66**, 125.
21 G. M. Sheldrick, *Acta Crystallogr*., 2015, **A71**, 3.
22 G. M. Sheldrick, *Acta Crystallogr*., 2015, **C71**, 3.
23 O. V. Dolomanov, L. J. Bourhis, R. J. Gildea, J. A. K. Howard and H. Puschmann. *J. Appl. Crystallogr.*, 2009, **42**, 339.
24 T. Kawase, T. Fujiwara, C. Kitamura, A. Konishi, Y. Hirao, K. Matsumoto, H. Kurata, T. Kubo, S. Shinamura, H. Mori, E. Miyazaki and K. Takimiya, *Angew. Chem., Int. Ed.*, 2010, **49**, 7728.
25 H. Zhang, T. Karasawa, H. Yamada, A. Wakamiya and S. Yamaguchi, *Org. Lett.*, 2009, **11**, 3076.
26 M. Saito, M. Nakamura and T. Tajima, *Chem. – Eur. J.*, 2008, **14**, 6062.
27 T. Maekawa, Y. Segawa and K. Itami, *Chem. Sci.*, 2013, **4**, 2369.

Received: 14th March 2022; Com. 22/6828